OpenProp: An Open-source Parametric Design and Analysis Tool for Propellers

Brenden Epps[1], Julie Chalfant[2], Richard Kimball[3], Alexandra Techet[4], Kevin Flood[1], and Chrysssostomos Chryssostomidis[5]
1: Graduate Student, MIT Mechanical Engineering
2: Research Scientist, MIT Sea Grant College Program
3: Assistant Professor of Engineering, Maine Maritime Academy and corresponding author: (kimball@mma.edu)
4: Associate Professor, MIT Mechanical Engineering
5: Director, MIT Sea Grant College Program and Professor, MIT Mechanical Engineering

Keywords: OpenProp, propeller design, propeller analysis

Abstract

OpenProp is an open-source computational tool for the design and analysis of optimized propellers and turbines. The numerical model is based on the vortex lattice lifting line methods utilized by the US Navy as well as commercial designers. The code is written in MATLAB M-code, which is widely used in academia and industry. The code includes analysis capability to estimate the performance curve of a given design for use in off-design performance prediction. In addition, a module to generate cavitation bucket diagrams for cavitation analysis is presented. Examples of designs are presented including validation comparisons and examples of actual parts fabricated from the code using 3D printing technology.

As a case study, we present the design and analysis of a propeller for an electrically-driven destroyer-sized twin-screw vessel. Herein, we explore the redesign of a propeller for a higher shaft rotation rate, in order to investigate the impacts on motor sizing within the limits of cavitation. Off-design propeller performance is also predicted to aid in modeling the hydrodynamic performance and fuel usage of the ship operating over its typical operational profile.

1. INTRODUCTION

OpenProp is a suite of open-source propeller and turbine design codes written in the MATLAB programming language [Kimball et. al. 2008]. The codes are based on the same propeller design theory utilized in codes employed by the US Navy for parametric design of marine propellers [Kerwin 2007]. OpenProp is designed to be a GUI-based user-friendly tool that can be used by both propeller design professionals as well as novices to propeller design.

A team of researchers at MIT, Maine Maritime Academy and University of Maine have contributed to the current OpenProp code. OpenProp began in 2001 with the propeller code PVL developed by Kerwin [2007] as part of his MIT propeller design course notes. The first MATLAB version of this code, MPVL, incorporated graphical user interfaces for parametric design and preliminary bladerow design [Chung 2007]. Geometry routines were later added which interfaced with the CAD program Rhino to generate a 3D printable propeller [D'Epagnier et. al. 2007]. These early codes were capable of designing propellers using a simple Lerb's criteria optimizer routine [Lerbs 1952]. Using a generalized optimizer routine implemented by Epps [2009], the code was then extended to design ducted propellers [Stubblefield 2008].

This paper presents the methodology and numerical implementation of both the propeller design and analysis capabilities. OpenProp utilizes a vortex-lattice lifting-line representation of the blades with constant-diameter helical vortices to represent the blade wake. The computational model incorporates a standard wake alignment procedure to accurately represent moderate blade loading. As such, it can design both propellers and axial flow turbines using the same numerical representation [Epps et. al. 2009], although only propeller design is discussed herein. The code also has an analysis capability to estimate the performance curve of a given design for use in off-design evaluation, which will be described herein.

The long term goal of the OpenProp project is to provide a user-friendly, accurate, and validated open-source code that can be used to design and prototype a variety of propellers and turbines including:

- Marine Propellers (free tip and ducted)
- Marine Hydrokinetic Turbines (free tip and ducted)
- Hydraulic turbines

The OpenProp team is currently integrating and validating several new features into the OpenProp code. Implementation of the turbine design module is in validation stages. Coupling with the open-source code XFOIL [Drela 1989] is also underway, which will give OpenProp flexibility in designing and analyzing blades with arbitrary foil shapes. Integration of the cavitation prediction tools presented herein is also underway. Future additions will include enhanced CAD and CAM modeling, strength analysis and coupling with electric motor parametric design and analysis. Visit the OpenProp website (http://openprop.mit.edu) for more information.

1.1. Data flow

OpenProp uses data structures to store the **input** parameters, **design**, **geometry**, and operating **states** of a propeller. The data flow is illustrated in figure 1. The **input** data (diameter, rotation rate, etc.) are defined by the user either though the GUI or by running a short script. The ***optimizer*** module determines the optimum propeller design, for the given inputs. The resulting propeller **design** can then be analyzed at off-design conditions (i.e. user-specified tip speed ratios) in the ***analyzer*** to determine off-design operating **states**. The ***crafter*** can determine the 3D **geometry** and prepare rapid prototyping files for production of the propeller.

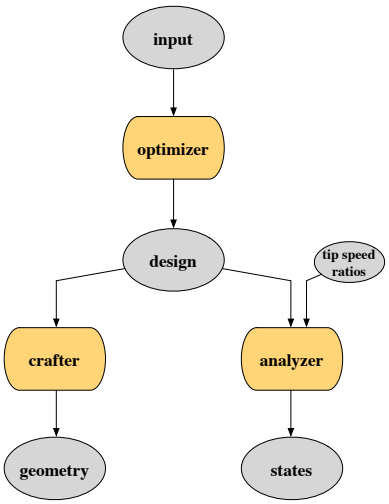

Figure 1. OpenProp information flow chart

2. METHODOLOGY

The following is the theoretical foundation and an overview of the numerical implementation of the OpenProp propeller/turbine design code . It draws from the theory presented in [Kerwin 2007, Coney 1989, Carlton 1994].

OpenProp is based on *moderately-loaded lifting line theory*, in which a propeller blade is represented by a lifting line, with trailing vorticity aligned to the local flow velocity (i.e. the vector sum of free-stream plus induced velocity). The induced velocities are computed using a vortex lattice, with helical vortex filaments trailing into the wake at discrete stations along the blade. The blade itself is modeled as discrete sections, having 2D section properties at each radius. Loads are computed by integrating the 2D section loads over the span of the blade. The goal of the propeller optimization procedure is to determine the optimum circulation distribution along the span of the blade, which yields the best performance (minimum torque for a specified thrust), given the inflow conditions and blade 2D section properties.

2.1. Propeller representation

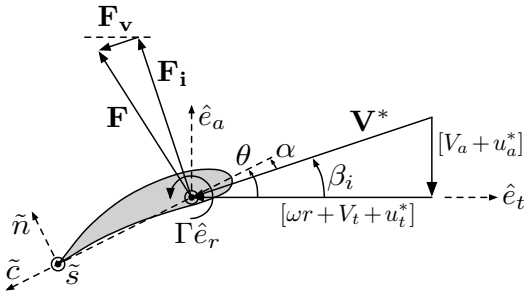

Figure 2. Propeller velocity/force diagram, as viewed from the tip towards the root of the blade. All velocities are relative to a stationary blade section at radius r.

The velocity/force diagram shown in figure 2 illustrates the velocities and forces (per unit span) on a 2D blade section in the axial $\hat{e}_a$ and tangential $\hat{e}_t$ directions. The propeller shaft rotates with angular velocity $\omega\hat{e}_a$, such that the apparent tangential (swirl) inflow at radius r is $-\omega r\hat{e}_t$. Also shown on figure 2 are the axial and tangential inflow velocities, $\mathbf{V_a} = -V_a\hat{e}_a$ and $\mathbf{V_t} = -V_t\hat{e}_t$; induced axial and tangential velocities, $\mathbf{u_a^*} = -u_a^*\hat{e}_a$ and $\mathbf{u_t^*} = -u_t^*\hat{e}_t$ (note that typically $u_t^* < 0$ when using this definition, so $\mathbf{u_t^*}$ actually points in the $\hat{e}_t$ direction); and the total resultant inflow velocity, $\mathbf{V}^*$, which has magnitude

$$V^* = \sqrt{(V_a+u_a^*)^2+(\omega r+V_t+u_t^*)^2} \tag{1}$$

and is oriented at pitch angle,

$$\beta_i = \tan^{-1}\left[\frac{V_a+u_a^*}{\omega r+V_t+u_t^*}\right] \tag{2}$$

to the $\hat{e}_t$ axis. Also shown on figure 2 are the angle of attack, α; blade pitch angle $\theta = \alpha+\beta_i$; circulation, $\Gamma\hat{e}_r$; (inviscid) Kutta-Joukowski lift force, $\mathbf{F_i} = \rho\mathbf{V}^*\times(\Gamma\hat{e}_r)$; and viscous drag force, $\mathbf{F_v}$, aligned with $\mathbf{V}^*$. Assuming the Z blades are identical, the total thrust and torque on the propeller are

$$\mathbf{T} = Z\int_{r_h}^{R}[F_i\cos\beta_i - F_v\sin\beta_i]dr\ (\hat{e}_a) \tag{3}$$

$$\mathbf{Q} = \rho Z\int_{r_h}^{R}[F_i\sin\beta_i + F_v\cos\beta_i]rdr\ (-\hat{e}_a) \tag{4}$$

where $F_i = \rho V^*\Gamma$ and $F_v = \frac{1}{2}\rho(V^*)^2C_Dc$ are the magnitudes of the inviscid and viscous force per unit radius, ρ is the fluid density, C_D is the drag coefficient, c is the section chord, and r_h and R are the radius of the hub and blade tip, respectively.

The efficiency of the propeller is the ratio of useful power produced by the propeller to the input shaft power, $\eta = \frac{TV_s}{Q\omega}$, where V_s is the ship speed (i.e. free-stream speed).

2.2. Vortex lattice formulation

OpenProp employs a standard propeller vortex lattice model to compute the axial and tangential induced velocities, $\{u_a^*, u_t^*\}$. In this formulation, a Z-bladed propeller is modeled as a single representative radial lifting line, partitioned into M panels. A horseshoe vortex filament with circulation $\Gamma(i)$ surrounds the i^{th} panel, consisting of constant-pitch helical trailing vortex filaments at the panel endpoints ($r_v(i)$ and $r_v(i+1)$) and the segment of the lifting line that spans the panel. The induced velocities are computed at *control points* on the lifting line at radial locations $r_c(m)$, $m = 1 \ldots M$, by summing the velocity induced by each horseshoe vortex

$$u_a^*(r_c(m)) \equiv u_a^*(m) = \sum_{m=1}^{M} \Gamma(i)\bar{u}_a^*(m,i) \tag{5}$$

$$u_t^*(r_c(m)) \equiv u_t^*(m) = \sum_{m=1}^{M} \Gamma(i)\bar{u}_t^*(m,i) \tag{6}$$

where $\bar{u}_a^*(m,i)$ and $\bar{u}_t^*(m,i)$ are the axial and tangential velocity induced at $r_c(m)$ by a unit-strength horseshoe vortex surrounding panel i, These influence matrices are functions of $\{Z, r_c(m), r_v(i), \beta_i(i)\}$, which are computed using the approximations by Wrench [1957].

Following Kerwin [2007], the hub is modeled as an image vortex lattice, with the image trailing vortex filaments having equal and opposite strength as the real trailing vortex filaments and radii $r_{im}(i) = \frac{r_h^2}{r_v(i)}$. The image vorticity is shed through the trailing surface of the hub and rolls up into a *hub vortex* of radius, r_o. The drag due to the hub vortex is $D_h = \frac{\rho Z^2}{16\pi}\left[\ln\left(\frac{r_h}{r_o}\right)+3\right][\Gamma(1)]^2(-\hat{e}_a)$. For practical purposes, it suffices to set $\frac{r_h}{r_o} = 1$, which sets the logarithm to zero.

2.3. Propeller optimization module

Following Coney [1989], the propeller optimization problem is to find the set of M circulations of the vortex lattice panels that produce the least torque

$$Q = \rho Z \sum_{m=1}^{M} \left\{[V_a + u_a^*]\Gamma + \tfrac{1}{2}V^* C_D c[\omega r_c + V_t + u_t^*]\right\} r_c \triangle r_v \tag{7}$$

for a specified thrust, T_s,

$$T = \rho Z \sum_{m=1}^{M} \left\{[\omega r_c + V_t + u_t^*]\Gamma - \tfrac{1}{2}V^* C_D c[V_a + u_a^*]\right\} \triangle r_v - \text{Hflag} \cdot \frac{\rho Z^2}{16\pi}\left[\ln\left(\frac{r_h}{r_o}\right)+3\right][\Gamma(1)]^2 = T_s \tag{8}$$

where Hflag is set to 1 to model a hub or 0 for no hub. Here, $\{\rho, Z, \omega\}$ are constants and $\{\Gamma, u_a^*, u_t^*, V^*, c, V_a, V_t, C_D, r_c, \triangle r_v\}$ are evaluated at each control point radius, $r_c(m)$, in the summation. Note that $\{u_a^*, u_t^*, V^*\}$ are functions of the circulation distribution, Γ, by equations $\{(5),(6),(1)\}$.

The circulation optimization is performed using the method of the Lagrange multiplier from variational calculus. An auxiliary function, $H = Q + \lambda_1(T - T_s)$, is formed, where λ_1 is the unknown Lagrange multiplier that introduces the thrust constraint (8). Clearly, if $T = T_s$, then a minimum H coincides with a minimum Q. To find this minima, the derivatives with respect to the unknowns are set to zero, $\frac{\partial H}{\partial \Gamma(i)} = 0$ ($i = 1 \ldots M$) and $\frac{\partial H}{\partial \lambda_1} = 0$, which results in a system of $M+1$ equations for as many unknowns $\{\Gamma(i = 1 \ldots M), \lambda_1\}$. This non-linear system of equations is solved iteratively until convergence of the optimized circulation distribution, Γ, and flow parameters $\{u_a^*, u_t^*, \beta_i, \bar{u}_a^*, \bar{u}_t^*, V^*\}$.

The generalized circulation optimizer described herein was implemented in OpenProp by Epps [2009]. Stubblefield [2008] validated the optimizer for unducted and ducted cases against the U.S. Navy code PLL with good agreement in circulation distribution over a wide range of duct loadings.

2.4. Geometry module

Once the design operating state of the propeller/turbine is known, the geometry can be determined to give such performance. The 3D geometry is built from given 2D section profiles that are scaled and rotated according to the design lift coefficient, chord, and inflow angle $\{C_{L_0}, c, \beta_{i_0}\}$.

A given 2D section profile includes camber and thickness normalized by the chord, $\{\widetilde{f}/c, \widetilde{t}/c\}$, ideal angle of attack, $\widetilde{\alpha}_I$, and ideal lift coefficient, $\widetilde{C}_{L_I}$. Note that $\{\widetilde{f}, \widetilde{\alpha}_I, \widetilde{C}_{L_I}\}$ scale linearly with the maximum camber, $\widetilde{f}_0$ [Abbott and Von Doenhoff 1959]. The section lift coefficient is given in terms of the geometry by

$$C_L = 2\pi(\alpha - \alpha_I) + C_{L_I} \tag{9}$$

for $\alpha < \alpha_{\text{stall}}$, and the stall model is described in [Epps et. al. 2009]. In the geometry module, the angle of attack of each blade section is set to the ideal angle of attack ($\alpha = \alpha_I$) to prevent leading edge flow separation and/or cavitation. The lift coefficient (9) then becomes the ideal lift coefficient ($C_L = C_{L_I}$). In order to achieve the desired lift coefficient, C_{L_0}, the given $\widetilde{C}_{L_I}$ is scaled by scaling the section camber. Thus, the desired lift coefficient and section geometry is

$$\{C_L, f_0, f, \alpha_I\} = \frac{C_{L_0}}{\widetilde{C}_{L_I}} \cdot \{\widetilde{C}_{L_I}, \widetilde{f}_0, \widetilde{f}, \widetilde{\alpha}_I\} \tag{10}$$

The pitch angle of the blade section is then fixed at

$$\theta = \alpha_I + \beta_{i_0} \tag{11}$$

With this computed blade 2D section geometry, OpenProp can then form 3D renderings or export files for rapid prototyping of physical parts.

2.5. Performance analysis module

This section details the analysis of a propeller operating at an off-design (*OD*) tip-speed ratio,

$$\lambda_{OD} = \frac{\omega_{OD} R}{V_s} \tag{12}$$

An off-design operating state is defined by λ_{OD} and unknown flow parameters $\{V^*, \alpha, C_L, \Gamma, u_a^*, u_t^*, \beta_i, \bar{u}_a^*, \bar{u}_t^*\}$.

To proceed, we need equations for the angle of attack, α, and circulation, Γ. In the analyzer, the pitch angle, θ, of each blade section is fixed, so the net angle of attack is

$$\alpha - \alpha_I = \beta_{i_0} - \beta_i \tag{13}$$

The circulation can be computed from the 2D section lift coefficient, which is given in terms of the loading by

$$C_L = \frac{2\Gamma}{V^* c} \tag{14}$$

For a computed operating state to be physically-realistic, the above flow parameters must all be self-consistent. That is, equations {(1), (13), (9), (14), (5), (6), (2)} and the Wrench (1957) formulae must all hold, given λ_{OD}.

Since there are M vortex panels, there are $7M + 2M^2$ unknowns and a system of $7M + 2M^2$ non-linear equations that govern the state of the system. This system is solved in OpenProp using an approach similar to a Newton solver. During each iteration of the analyzer, one Newton solver iteration is performed to drive the residual vector

$$\mathbf{R} = \begin{bmatrix} V^* - \sqrt{(V_a + u_a^*)^2 + (\omega_{OD} r_c + V_t + u_t^*)^2} \\ \alpha - (\alpha_I + \beta_{i_0} - \beta_i) \\ C_L - (2\pi(\alpha - \alpha_I) + C_{L_I}) \\ \Gamma - \left(\frac{1}{2} C_L V^* c\right) \\ u_a^* - [\bar{u}_a^*] \cdot [\Gamma] \\ u_t^* - [\bar{u}_t^*] \cdot [\Gamma] \end{bmatrix} \tag{15}$$

towards zero. Given the new values of $\{V^*, \alpha, C_L, \Gamma, u_a^*, u_t^*\}$, the parameters $\{\beta_i, \bar{u}_a^*, \bar{u}_t^*\}$ are then updated. These new values are used in the next Newton iteration, and so on. This process repeats until convergence of the entire system. Since the method updates both $\{V^*, \alpha, C_L, \Gamma, u_a^*, u_t^*\}$ and $\{\beta_i, \bar{u}_a^*, \bar{u}_t^*\}$ in each iteration, it accounts for the coupled interaction between all $7M + 2M^2$ unknown flow parameters and converges on physically-realistic operating states [Epps et. al. 2009].

For each operating state, the analyzer computes the propeller thrust, torque, and power coefficients and the efficiency.

The OpenProp analyzer was validated with *U.S. Navy propeller 4119*. Figure 3 shows the circulation distribution of an OpenProp-designed version of 4119, showing good agreement with the design circulation distribution and off-design performance curves, as compared with U.S. Navy code PBD and experimental data from [Black 1997].

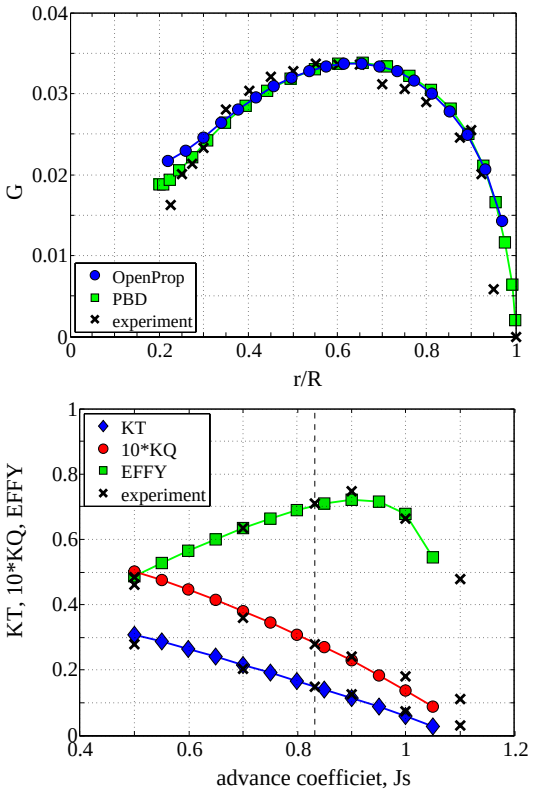

Figure 3. (top) Design circulation distribution for U.S. Navy propeller 4119. (bottom) Performance curves for propeller 4119. OpenProp results agree with PBD code solution and experimental data from [Black 1997].

2.6. Cavitation analysis module

This section details the preliminary cavitation analysis capabilities of OpenProp. Analysis of blade section cavitation requires the 2D foil pressure distribution, which is found in OpenProp using either of two 2D foil solvers. Peterson [2008] developed a cavitation analysis module using the open-source code XFOIL by Drela [1989]. For the present work, a simpler 2D vortex lattice code VLM by Chung [2007] was used as the 2D foil solver engine. The pressure distribution results are incorporated in a module that generates cavitation bucket diagrams for a given blade design. An example Brockett diagram is shown in figure 4. These diagrams can be generated for each 2D blade section, given the section meanline form and camber ratio. Using the Brockett diagram, the thickness ratio can be chosen to give adequate on-design cavitation margin and off-design angle of attack margin. The 2D solvers can also be used to analyze the blade pressure coefficient (C_P) distributions for determining cavitation margin and location by comparing the C_P values to the local cavitation number of the section (σ), as discussed later in this paper.

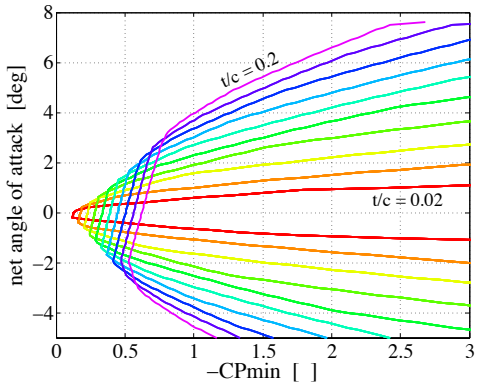

Figure 4. Brockett diagram (inviscid cavitation bucket diagram) for an example propeller with a NACA a=0.8 meanline and NACA66 thickness ($f_0/c = 0.0093$, $\triangle\alpha = 0.1°$).

3. CASE STUDY: ELECTRIC SHIP PROPELLER REDESIGN

We present as a case study, the redesign of a marine propeller for an electrically-driven ship. In this redesign, we consider a much higher shaft rotation rate in order to explore the implications on the propeller performance; electric motor design [see Englebretson et. al. 2009]; and ship hydrodynamics [see Chalfant and Chryssostomidis 2009]. Specifications for the *old* and *new* propellers are listed in tables 1 and 2.

Table 1. Specifications. For both propellers, the design ship speed is $V_s = 20$ [knots] $= 10.290$ [m/s]; the required thrust is $T_s = 4.2038 \times 10^5$ [N]; the sea-water density is $\rho = 1026$ [kg/m^3]; and the viscous drag coefficient is $C_D \approx 0.009$.

	old	*new*
Z	5	4
D [m]	5.1816	4.2672
D_{hub} [m]	1.7282	0.8534
N [rpm]	91.900	150
$J_s = \frac{V_s}{nD}$	1.2965	0.9646
$C_{T_s} = \frac{T_s}{\frac{1}{2}\rho V_s^2 \frac{\pi D^2}{4}}$	0.3670	0.5411
$K_{T_s} = \frac{T_s}{\rho n^2 D^4}$	0.2422	0.1977

3.1. Design optimization

OpenProp was used to design optimized propellers that meet the *old* and *new* design specifications. As a validation case, the U.S. Navy code PLL was also used to design an optimized propeller for the *old* specifications. These designs are characterized by their circulation distribution, thrust coefficient, C_T or K_T, torque coefficient, C_Q or K_Q, and efficiency, η. For reference, the efficiency of an actuator disc with $C_{T_s} = \{0.3670, 0.5411\}$ is $\eta = \frac{2}{1+\sqrt{1+C_{T_s}}} = \{0.9220, 0.8923\}$.

Table 2. Propeller input geometry. In both cases, all sections have a NACA a=0.8 meanline (which has $\widetilde{f}_0/c = 0.0679$, $\widetilde{C}_{L_I} = 1.0$, and $\widetilde{\alpha}_I = 1.54°$), and a NACA 65A010 thickness profile with $\widetilde{t}_0/c = 0.0200$.

Old propeller:			New propeller:		
r/R	c/D	V_A	r/R	c/D	V_A
0.3333	0.1852	0.9342	0.2000	0.2454	0.7300
0.3704	0.2447	0.9573	0.2500	0.2595	0.8200
0.4444	0.2847	0.9864	0.3000	0.2735	0.9000
0.5185	0.3518	1.0018	0.4000	0.3014	0.9700
0.5926	0.4242	1.0003	0.5000	0.3290	1.0000
0.6667	0.5549	0.9996	0.6000	0.3564	1.0000
0.7407	0.5314	1.0002	0.7000	0.3833	1.0000
0.8148	0.4323	1.0000	0.8000	0.4092	1.0000
0.8889	0.3387	1.0000	0.9000	0.4381	1.0000
0.9630	0.1889	1.0000	0.9500	0.4376	1.0000
1.0000	0.0020	1.0000	1.0000	0.0020	1.0000

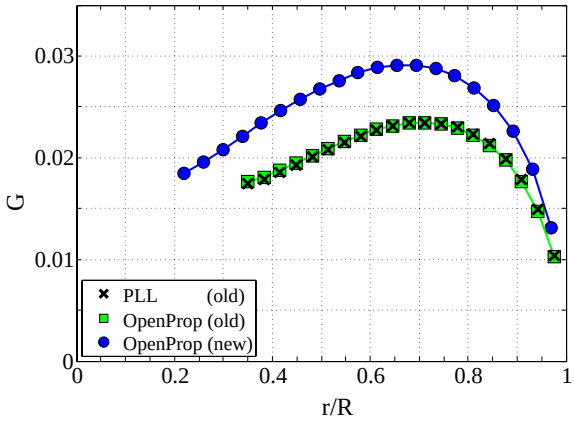

Figure 5. Normalized circulation, $G = \frac{\Gamma}{2\pi R V_s}$, versus radius for the *old* and *new* propellers.

The optimized circulation distributions are shown in figure 5. Both the PLL and OpenProp *old* propeller circulation distributions are nearly identical. These designs also have nearly identical computed performance data shown in table 3, which validates the OpenProp optimizer with PLL.

The optimized circulation distribution for the *new* propeller is also shown in figure 5. Although the blade loading, Γ, is similar for the two cases, the non-dimensional circulation, $G = \frac{\Gamma}{2\pi R V_s}$, is higher for the *new* propeller, due to the smaller propeller diameter. The smaller diameter also results in a slightly higher C_T and lower η, as expected.

The computed on-design propeller performance parameters of the *old* and *new* propellers are shown in table 3. In both cases, the efficiency is slightly lower than that predicted by actuator disc theory, since these propellers have a finite number of blades and since viscous forces are considered.

Table 3. Computed propeller performance at design (20 kts).

	old PLL	old OpenProp	new OpenProp
$J_s = \frac{V_s}{nD}$	1.2960	1.2965	0.9646
$C_T = \frac{T}{\frac{1}{2}\rho V_s^2 \frac{\pi D^2}{4}}$	0.3680	0.3670	0.5411
$C_Q = \frac{Q}{\frac{1}{2}\rho V_s^2 \frac{\pi D^3}{8}}$	0.2130	0.2123	0.2364
$K_T = \frac{T}{\rho n^2 D^4}$	0.2427	0.2422	0.1977
$K_Q = \frac{Q}{\rho n^2 D^5}$	0.0703	0.0701	0.0432
$\eta = \frac{J_s}{2\pi}\frac{K_T}{K_Q}$	0.7100	0.7109	0.6923

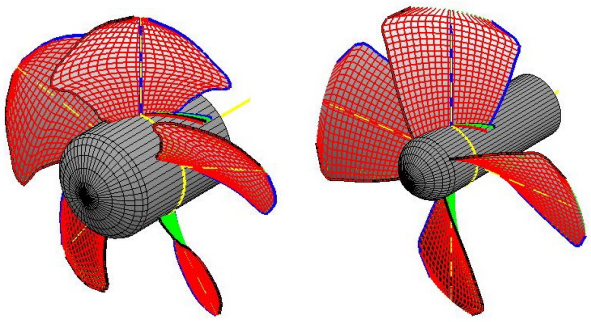

Figure 6. 3D geometry rendering: (left) *old* propeller, (right) *new* propeller. Since the present implementation of OpenProp does not treat propeller skew, these 3D renderings are skew-free, although skew was used in the *old* propeller design.

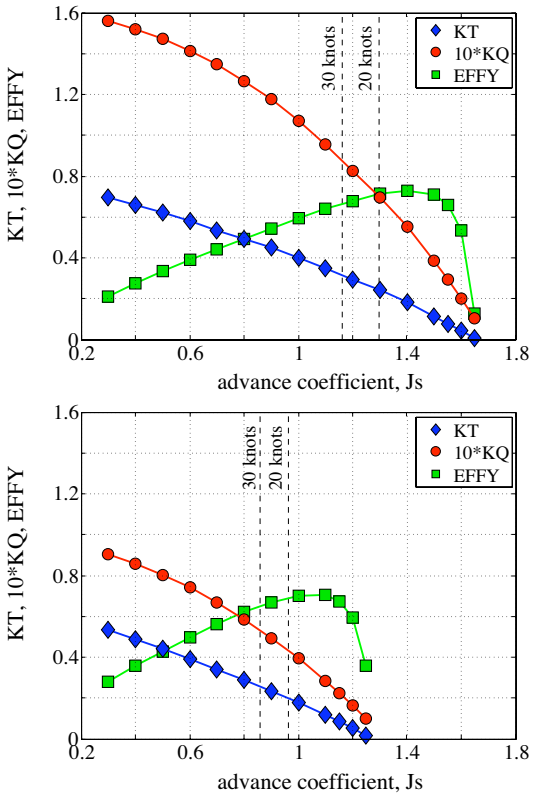

Figure 7. Performance curves for the *old* (top) and *new* (bottom) propellers.

Figure 6 shows a 3D rendering of the *old* and *new* propellers, as generated by OpenProp. OpenProp can also generate files for CAD and rapid prototyping, although prototypes were not manufactured for the present study.

3.2. Performance analysis

The performance curves for the *old* and *new* propellers are shown in figure 7. This figure highlights the performance at the design-intent *endurance speed* (20 knots) and the *maximum speed* of the ship (30 knots). Since both the endurance and maximum speed conditions are design criteria for this vessel, these data allow us to analyze the propeller performance at these operating conditions and enable ship system-level analysis, such as electric motor performance [see Englebretson et. al. 2009], fuel requirements, and ship hydrodynamic performance [see Chalfant and Chryssostomidis 2009].

In addition to the information shown in these plots, the flow parameters at any 2D blade section and any operating state can be extracted for cavitation analysis.

3.3. Cavitation analysis

Figure 8 shows the blade section cavitation analysis for the *old* and *new* propellers at $r/R = 0.7$ for the endurance speed (20 knots) and maximum speed (30 knots). This figure shows that this blade section of the *old* propeller is marginally cavitation free at the endurance speed and has substantial back cavitation at the maximum speed.

Figure 8 also shows the cavitation performance of the *new* higher-speed redesigned propeller at 20 and 30 knots. Though the propeller performance of the redesigned propeller was acceptable, the cavitation at 30 knots is clearly unacceptable, since this detailed cavitation analysis shows significant face cavitation would occur at this speed.

Since the *new* propeller had significant cavitation, a *second iteration* of the propeller redesign was performed, with a design rotation rate of 120 RPM at the endurance speed (20 kts). Figure 9 shows that this *second-iteration* propeller had little or no face cavitation when operated at maximum speed (30 kts) and that it had similar efficiency and thrust performance to the previous design. Using the OpenProp tools, additional redesign and analysis can be performed rapidly.

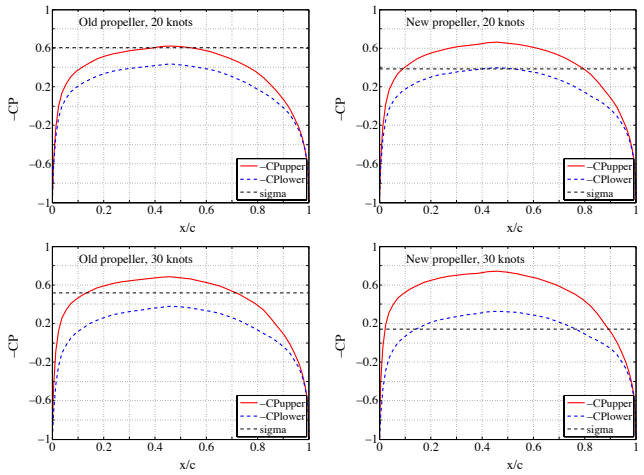

Figure 8. Pressure coefficient versus chordwise coordinate for the *old* and *new* propeller at the endurance (20 kts) and maximum (30 kts) speeds.

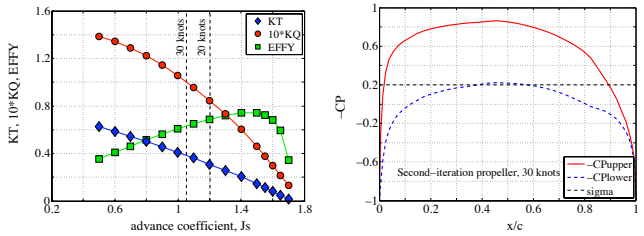

Figure 9. Performance curves and pressure distribution for a *second-iteration* design derived from the *new* propeller, but with a design rotation rate of 120 RPM.

4. CURRENT RESEARCH FOCUS

OpenProp is a continuing work in progress, but has reached the level of development where it has been useful to those not directly involved with the code. It brings the considerable power of vortex lattice analysis to the fingertips of novice and expert propeller designers with its friendly GUI and higher-power command-line interfaces.

In the present version of OpenProp, users have the option of working through the MATLAB command line or the graphical user interface (GUI). The GUI provides a parametric analysis interface for preliminary design and a single propeller interface for detail design (shown in figure 10). Both modes take basic parameters such as the diameter, number of blades, ship speed, etc. In the design optimizer, OpenProp uses these inputs to generate a vortex lattice model of the propeller and optimizes the circulation distribution on this model. With this design, OpenProp can then craft the geometry required to produce such performance, and OpenProp can also analyze the propeller in off-design operating conditions.

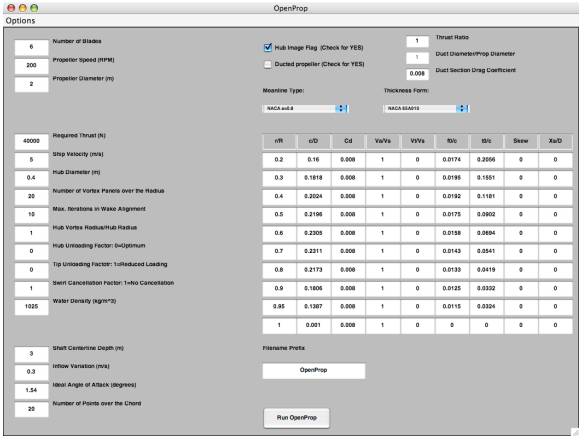

Figure 10. OpenProp graphical user interface.

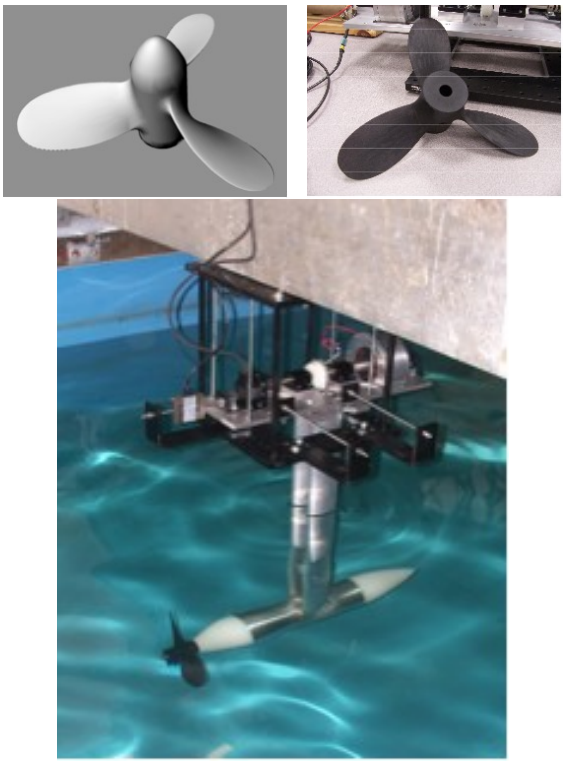

Figure 11. OpenProp rendering, 3D printed model, and tow-tank testing of propeller OP4148.

D'Epagnier [2007] designed and built a propeller to emulate the performance of *U.S. NAVY propeller 4148* [Kinnas 1995] as a test case for OpenProp. Figure 11 shows the propeller as designed and rendered in Rhino, the physical 3D printed propeller, and the propeller as it was undergoing tests at the tow tank at the University of Maine at Orono at the time of publication.

OpenProp is also a valuable teaching and educational tool, allowing students to learn the fundamentals of propeller design and become familiar with the physical models and numerical methods used in the field. Though hands on learning modules, OpenProp can be readily integrated into the classroom for both undergraduate and advanced graduate subjects. Modules are currently under development for MIT undergraduate course 2.016 Hydrodynamics and graduate course 2.23 Hydrofoils and Propellers, and roll-out is planned for the fall 2009 semester.

Efforts currently underway with the OpenProp code development include improvements to the GUI, verification testing of the turbine optimizer, and experimental validation testing of OpenProp propeller and turbine designs. Future additions to OpenProp are planned in the following areas:

- Integration of the 2D foil code XFOIL for arbitrary geometries and inclusion of viscous boundary layer effects,
- Integration of the cavitation bucket generator of Peterson (2008) into the OpenProp code,
- Addition of multiple blade row design capability,
- Addition of blade strength analysis capability,
- Extension of blade outputs to CAD programs such as SolidWorks, and internal generation of 3D print files.
- Development of hands-on learning modules for use in undergraduate and graduate level classes.

The goal of the OpenProp team is to provide accurate and powerful propeller and axial flow turbine design codes for use by both novice users and experienced designers. The open-source nature of the code (published under the GNU public License protocol) is intended to be a public resource to enhance the art of propeller design and analysis.

Acknowledgments This work is supported by the Office of Naval Research N000140810080, ESRDC Consortium and MIT Sea Grant College Program, NA06OAR4170019. In addition, the authors wish to thank Mr. Robert S. Damus of the Project Ocean, who was instrumental in securing a fellowship that made some of this research possible. The authors also thank Professor Kerwin for providing us access to his propeller codes (PLL and PBD).

REFERENCE

Abbott, I. H., and Von Doenhoff, A. E. *Theory of Wing Sections*. Dover, 1959.

Black, S.D. "Integrated Lifting Surface/Navier-Stokes Design and Analysis Methods for Marine Propulsors". Ph.D. thesis. MIT, 1997.

Carlton, J. S. *Marine Propellers and Propulsion*. Butterworth-Heinemann, 1994.

Chalfant, J.S. and Chryssostomidis, C. "Toward the Development of an Integrated Electric Ship Evaluation Tool", Proc. Grand Challenges in Modeling and Simulation (GCMS09), Istanbul, Turkey. July 13-16, 2009.

Chung, H.-L. "An enhanced propeller design program based on propeller vortex lattice lifting line theory". M.S. thesis, MIT, 2007.

Coney, W.B. "A Method for the Design of a Class of Optimum Marine Propulsors". PhD thesis, MIT, 1989.

D'Epagnier, K.P.; Chung, H.-L.; Stanway, M.J.; and R.W. Kimball. "An Open Source Parametric Propeller Design Tool". Oceans 2007, p. 1-8, October 2007.

Drela, M. "XFOIL: An Analysis and Design System for Low Reynolds Number Airfoils." In: T.J. Mueller, editor. Low Reynolds Number Aerodynamics: Proceedings for the Conference, Notre Dame, Indiana, USA, 5-7 June 1989. Springer-Verlag, p. 1-12.

Epps, B.; Stanway, J.; and Kimball, R. "OpenProp: An Open-Source Design Tool for Propellers and Turbines," SNAME Propeller and Shafting conference, 2009.

Englebretson, S.C.; Kirtley Jr., J. L.; and Chryssostomidis, C. "Optimization of Direct Drive Induction Motors for Electric Ship Propulsion with High Speed Propellers", Proc. Grand Challenges in Modeling and Simulation (GCMS09), Istanbul, Turkey. July 13-16, 2009.

Flood, K. "Propeller Performance Analysis Using Lifting Line Theory", M.S. Thesis, MIT, 2009.

Kerwin, J.E. *Hydrofoils and Propellers*. MIT course 2.23 notes, 2007.

Kimball, R.W.; Epps, B.P.; and M.J. Stanway. OpenProp MATLAB code, http://openprop.mit.edu, 2008.

Kinnas, S.A. "University/Navy/Industry Consortium on Cavitation of High Speed Propulsors," fifth meeting, June 1st and 2nd, 1995.

Lerbs, H.W. "Moderately Loaded Propellers with a Finite Number of Blades and an Arbitrary Distribution of Circulation." Trans. SNAME, v. 60, 1952.

Peterson, C.J. "Minimum Pressure Envelope Cavitation Analysis Using Two-Dimensional Panel Method" M.S. Thesis, MIT, June 2008.

Stubblefield , J.M. "Numerically Based Ducted Propeller Desgin using Vortex Lattice Lifting Line Theory", M.S. Thesis, MIT, June 2008.

Wrench, J. W. "The calculation of propeller induction factors." Technical Report 1116, David Taylor Model Basin, February, 1957.